Liquid Crystals

Publication details, including instructions for authors and subscription information:
http://www.informaworld.com/smpp/title~content=t713926090

AFM investigations of a sample showing the B_2 phase

A. Hauser; H. Schmalfuss; H. Kresse

To cite this Article Hauser, A. , Schmalfuss, H. and Kresse, H.(2000) 'AFM investigations of a sample showing the B_2 phase', Liquid Crystals, 27: 5, 629 — 634

To link to this Article: DOI: 10.1080/026782900202471

URL: http://dx.doi.org/10.1080/026782900202471

Liquid Crystals, 2000, Vol. 27, No. 5, 629–634

AFM investigations of a sample showing the B_2 phase†

A. HAUSER, H. SCHMALFUSS and H. KRESSE*
Institut für Physikalische Chemie, Martin-Luther-Universität Halle-Wittenberg,
Mühlpforte 1, D-06108 Halle, Germany

(*Received 4 October 1999; accepted 29 November 1999*)

Atomic force microscopy (AFM) images reveal that the liquid crystalline B_2 phase has no helical superstructure, in contrast to the B_7 phase. This is demonstrated on comparing the AFM images of focal-conic domains in the smectic A, cholesteric, B_2 and B_7 phases. The B_2 and B_7 phases are phases formed by banana-shaped molecules. The results point to the existence of ferroelectric clusters with a random size distribution which also cause the low frequency dielectric relaxation.

1. Introduction

Dielectric investigations of the bulky banana-shaped molecules with the structure

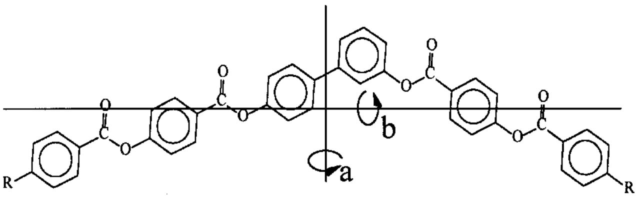

sample **1** $R = -C_{12}H_{25}$ M 351 B_2 429 I
sample **2** $R = -OC_{12}H_{25}$ Cr_1 355 Cr_2 379 B_2 432 I (all temperatures in K)

have shown that the reorientation of the molecules about the molecular long axis **b** does not follow a simple Arrhenius behaviour [1]. Therefore, the relaxation times τ_2 given in [1] were fitted to the Vogel–Fulcher–Tamann equation (figure 1)

$$\tau_2 = \tau_{2\infty} \exp[A/(T - T_V)]. \tag{1}$$

The Vogel temperature of $T_V = 307$ K obtained from the data between 340 and 385 K should result in a glass transition temperature T_g (calorimetric value) of about 347 K, because in most cases the difference $T_g - T_V$ is between 30 and 50 K [2].

The glass transition could not be detected by calorimetric measurements due to the transition into the M phase which is probably a solid modification [1]. Sample **2** shows the same behaviour, but in this case crystallization prevents measurements at lower temperatures. For the following experiments, it is only of interest that the expected glass temperature is above room temperature and that the B_2 phase can be frozen in. This gives us the chance to investigate the B_2 phase by atomic force microscopy (AFM). Such measurements are necessary to explain the second relaxation process in figure 1 characterised by τ_1. The low activation energy of $84 \pm 3\,\mathrm{kJ\,mol^{-1}}$ and the relatively high value of the dielectric increment do not allow this absorption to be interpreted in terms of reorientation of the molecules about the molecular short axes **a**. Furthermore the Cole–Cole distribution parameter of $\alpha_1 = 0.4$ found in the B_2 phase does not agree with the Debye process ($\alpha = 0$) seen for the low frequency absorption in another liquid crystal [3]. This points to a broad and statistical distribution of size of the collective units responsible for this absorption. Therefore, we used the AFM method to look for possible superstructures which can produce an additional dielectric response [4].

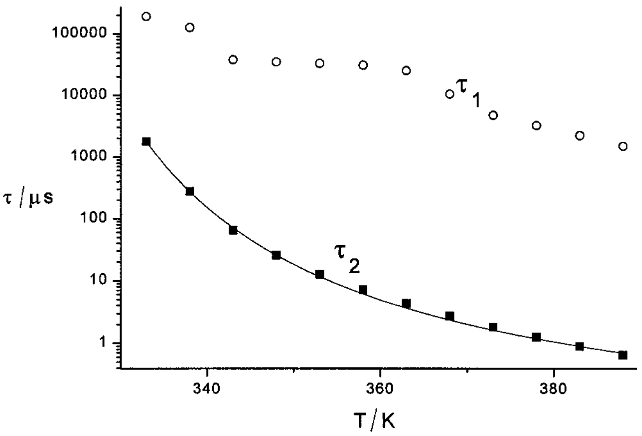

Figure 1. Dielectric relaxation times of **1**.

---

*Author for correspondence,
e-mail kresse@chemie.uni-halle.de

†Dedicated to the 75th birthday of Prof. Alfred Saupe.

Liquid Crystals ISSN 0267-8292 print/ISSN 1366-5855 online © 2000 Taylor & Francis Ltd
http://www.tandf.co.uk/journals

2. Experiments and results

The samples were filled into a 10 µm sandwich cell made of glass, heated to the clearing temperature and cooled to room temperature; the cover plate was then removed. In some cases the sample was melted directly on highly oriented pyrolytic graphite (HOPG). After that the substrate with the film was again heated to the clearing temperature and cooled to room temperature. AFM measurements were performed using the TMX 2000 Explorer and Discoverer Scanning Probe Microscope of Topometrix at room temperature and under ambient conditions. The images were obtained by the non-contact method (cantilever resonance frequency: ≈ 300 kHz).

First, AFM experimental data for a sitosterol ester showing the classical smectic A phase with focal-conic domains are presented [5, 6]. This sample is used as a reference for the discussion. Figure 2 shows the AFM image together with a cross-section through such focal-conic domains. Figure 3 displays a part of figure 2 with nearly hexagonal symmetry.

Such focal conic domains often occur in layered liquid crystalline structures [7, 8]. As early as 1910, Friedel and Grandjean had described focal-conic domains in anisotropic liquids [9]. These are defect structures with two singular lines in the centre of each domain [10]. The pair of singular lines (here a circle and a straight line) and the smectic layer structure in a focal-conic domain are sketched in figure 4. The molecules are oriented perpendicular to the concentric, equidistant smectic layers. The arrow in figure 4 indicates the funnel-shaped empty space which is also represented by the line profiles in figures 2 and 3 and in the following figures. The free surface shows a strong modulation by the focal-conic domains where the smectic layers are

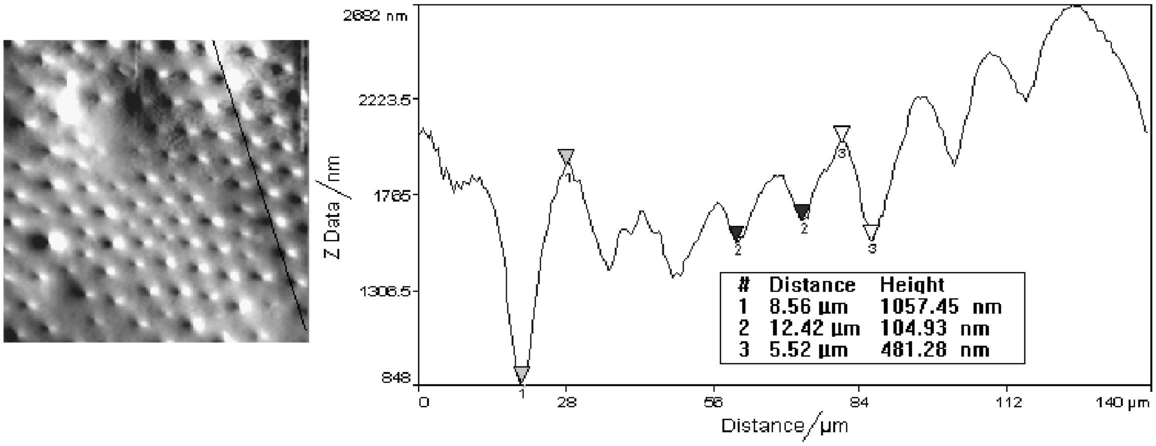

Figure 2. AFM image and line profile of focal-conic domains of the smectic A phase of a sitosterol ester. Inset data relate to the distance and height differences between points on the line indicated by differently numbered pairs of inverted triangles.

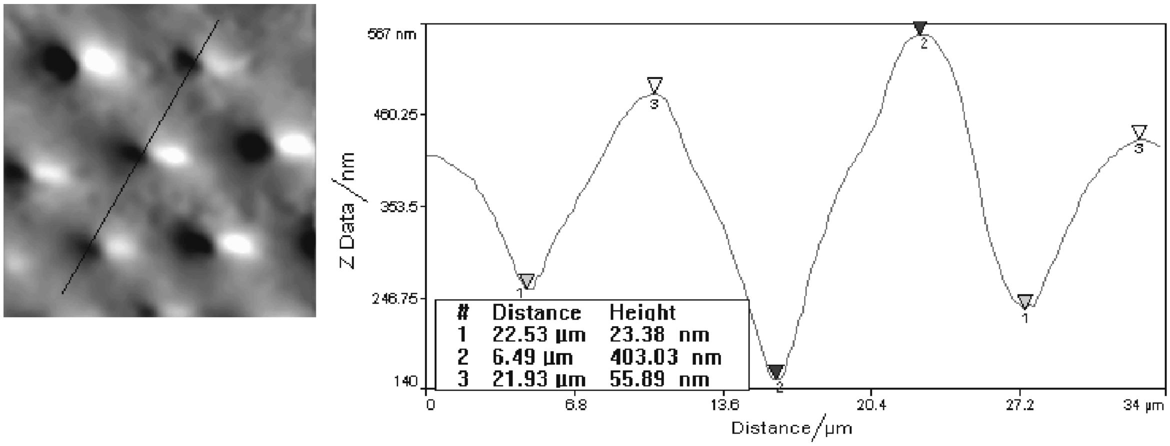

Figure 3. AFM image and cross section through focal-conic domains of a smectic A phase (detail of figure 2). Inset data are as described in the legend to figure 2.

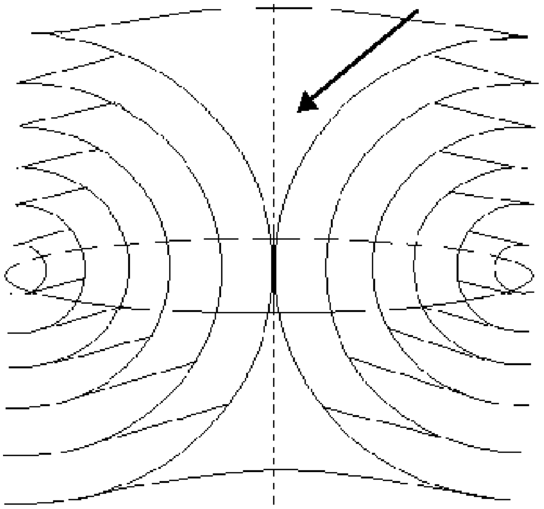

Figure 4. Smectic layer geometry in the vertical cross section of the toroidal focal-conic domain with a circle and a straight line as a pair of defect lines (dashed lines). The molecules are oriented perpendicular to the concentric, equidistant layers. The arrow indicates the funnel-shaped empty space as observed in figure 3.

deformed into Dupin cyclides with a funnel-shaped centre (defects with negative Gaussian curvature [8]) of about 1 µm depth (figure 2).

The funnel-shape of the focal-conic domains in the smectic A phase at elevated temperatures is observable by interference microscopy and is also preserved after cooling in the glassy state [6]. The distance between two focal-conic domains is about 12 µm (figure 2).

Similar AFM images were obtained for both samples showing the B_2 phase. Therefore, it can be concluded that the B_2 phase has a layered structure. This is in accordance with X-ray investigations [11]. Figure 5 shows focal-conic domains on a border area of a drop with a thickness of 5 µm of sample **2**. The depths of the focal-conics of about 200 nm and the distances of about 2 µm are only 16% of those observed in figure 3 where the scale is double in size relative to figure 5.

In order to see more details, a part of figure 5 is presented as figure 6 with a higher magnification. It is clearly recognized that, in contradiction to figures 2 and 3, additional defect lines connect the centres of singularities, reminding one of polygonal textures [7].

Sample **1** prepared on highly oriented pyrolytic graphite (HOPG) also shows focal-conic domains as presented in figures 7 and 8. The depths and the distances for the focal-conics are comparable to those of sample **2** in figures 5 and 6. The focal-conic domains are located along the edge dislocations.

The AFM image of figure 9 is reminiscent of 'broken massifs', but here also focal-conics occur with a diameter of about 2 µm and depth of 200 nm. The focal-conics are connected by defect lines as observed also in figures 4 and 5. These images were obtained after heating the sample to the clearing temperature and cooling at 0.2 K min^{-1}. In the line measurement beside the focal-conics (figure 9), steps of about 5.8 nm are recognizable, corresponding to the molecular length. These steps of one layer distance allow us to conclude that ferroelectric clusters exist in the B_2 phase. There is no evidence for a superstructure as, for example, observed in the focal-conic domains of the B_7 phase with regular stripes (see figure 10). Also, in this case, additional defect lines connecting the centres of singularities as in figures 5, 6 and 9 are observed. In figure 10 the general case of focal-conics is given for the B_7 phase where the defect lines are an ellipse and a hyperbola, which are not observable in the surface.

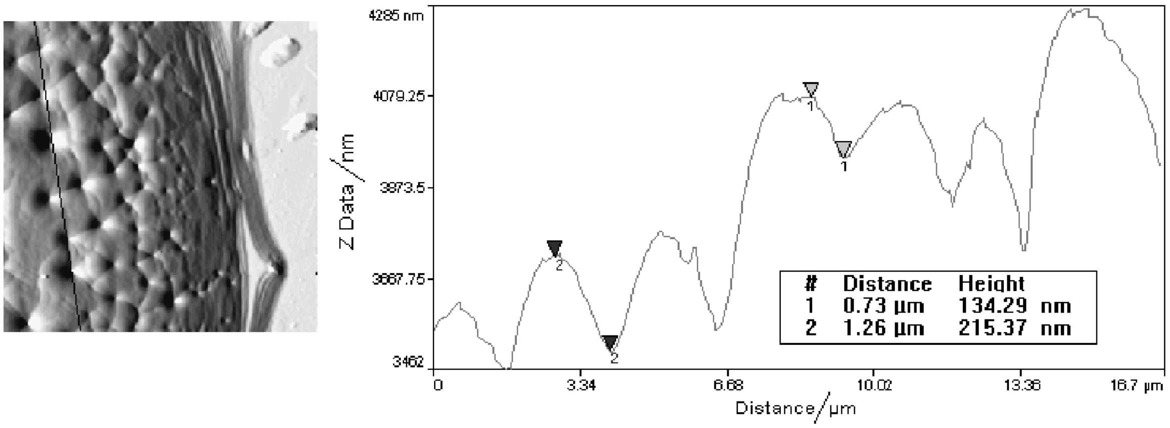

#	Distance	Height
1	0.73 µm	134.29 nm
2	1.26 µm	215.37 nm

Figure 5. AFM image and cross section of sample **2**. The focal-conic domains of the B_2 phase are located near to the border line of a drop. Inset data are as described in the legend to figure 2.

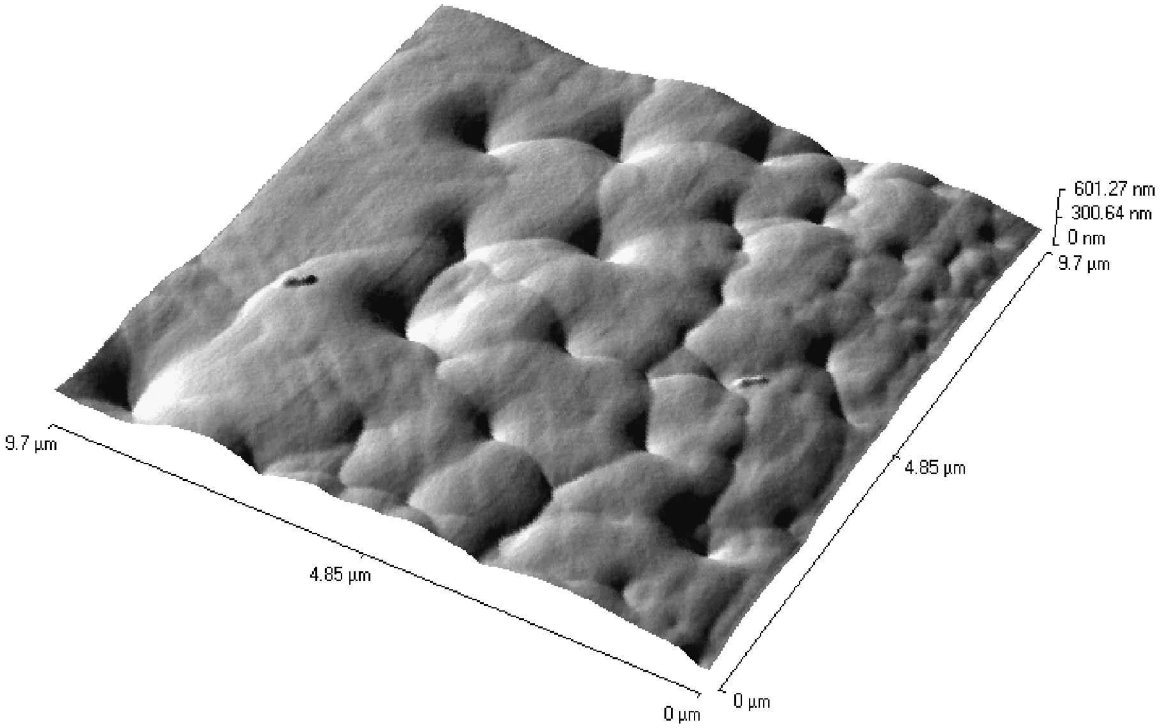

Figure 6. AFM image of a part of figure 5 with focal-conic domains of different size in the B_2 phase (sample **2**).

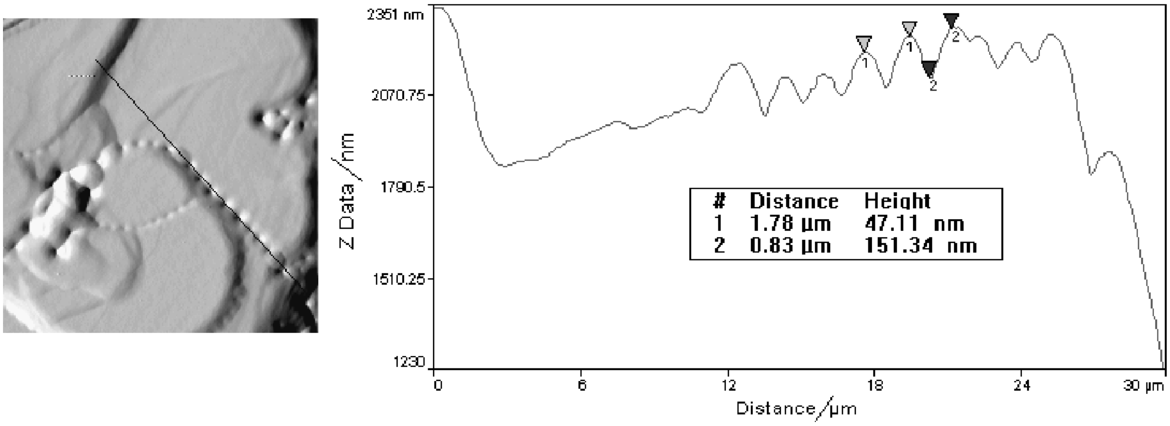

Figure 7. AFM image and line measurement along focal-conic domains in the B_2 phase of sample **1**. Inset data are as described in the legend to figure 2.

In order to illustrate the difference from a cholesteric phase, an AFM image (figure 11) of an oligomeric siloxane C4770L (g 329 N* 481 I, in K) produced by Wacker Chemie was reinvestigated [12]. Here the typical defect lines seen in the B_2 and B_7 phases do not appear.

3. Conclusions

Summarizing the results one can conclude the following. The low frequency absorption of the B_2 phase is not connected with a dielectric response of a regular superstructure. The B_2 phase shows focal-conic domains. Contrary to classical focal-conic domains, defect lines between the domains or images which are reminiscent of 'broken massifs' were detected. For this reason we interpret the low frequency dielectric response as the result of smaller ferroelectric clusters with a statistical size. This conclusion is supported by the relatively high value of the Cole–Cole distribution parameter seen by dielectric measurements.

We are indebted to Prof. C. Tschierske and Dipl. Chem. D. Shen for providing the samples, and also to DFG and the Fonds der Chemischen Industrie for financial support.

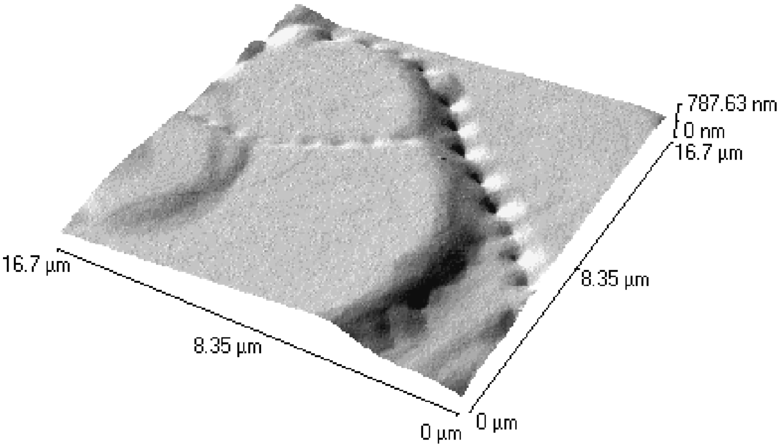

Figure 8. AFM image of the central part of figure 7 with lines of focal-conic domains in the B_2 phase (sample **1**).

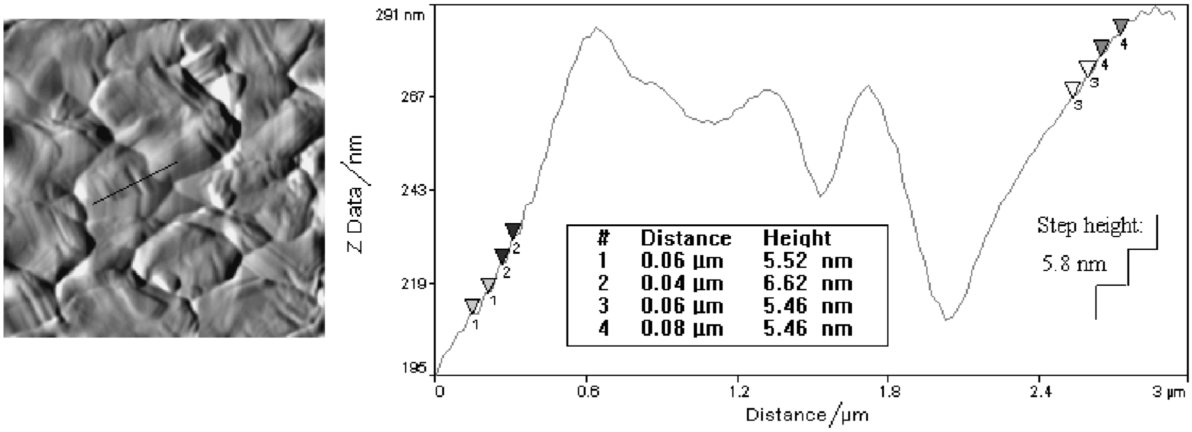

#	Distance	Height
1	0.06 µm	5.52 nm
2	0.04 µm	6.62 nm
3	0.06 µm	5.46 nm
4	0.08 µm	5.46 nm

Figure 9. AFM image and line measurement beside the focal-conic domains in the B_2 phase (sample **1**). The observed steps correspond to the molecular length. For a better understanding, the steps are sketched in the right hand side of the figure giving the line measurements. Inset data are as described in the legend to figure 2.

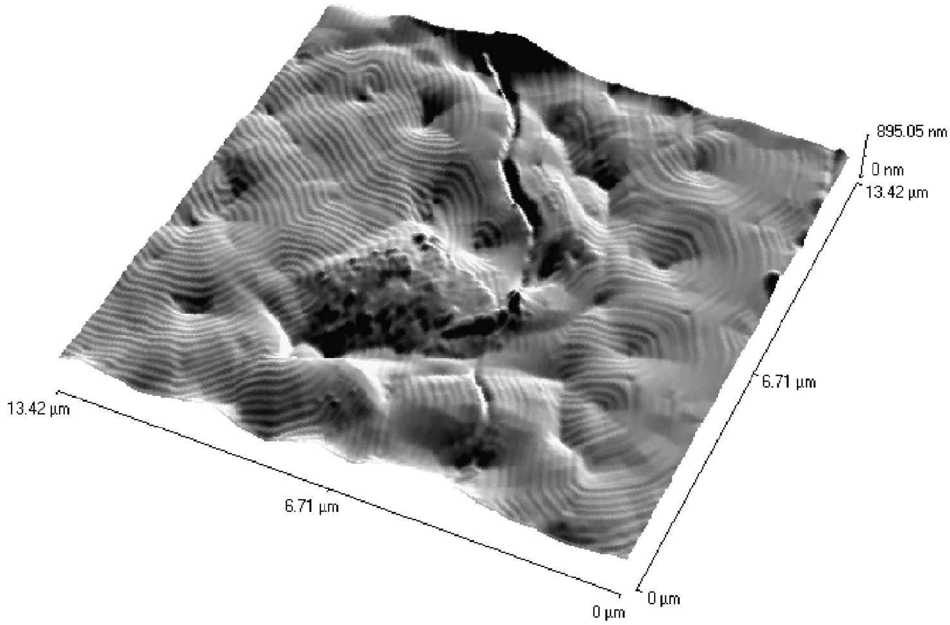

Figure 10. AFM image representing a superstructure of the B_7 phase with focal-conic domains (depth ≈ 300 nm) modulated by periodic lines with a distance of 220 nm and a height of 15 nm (see sample 2 in [4]).

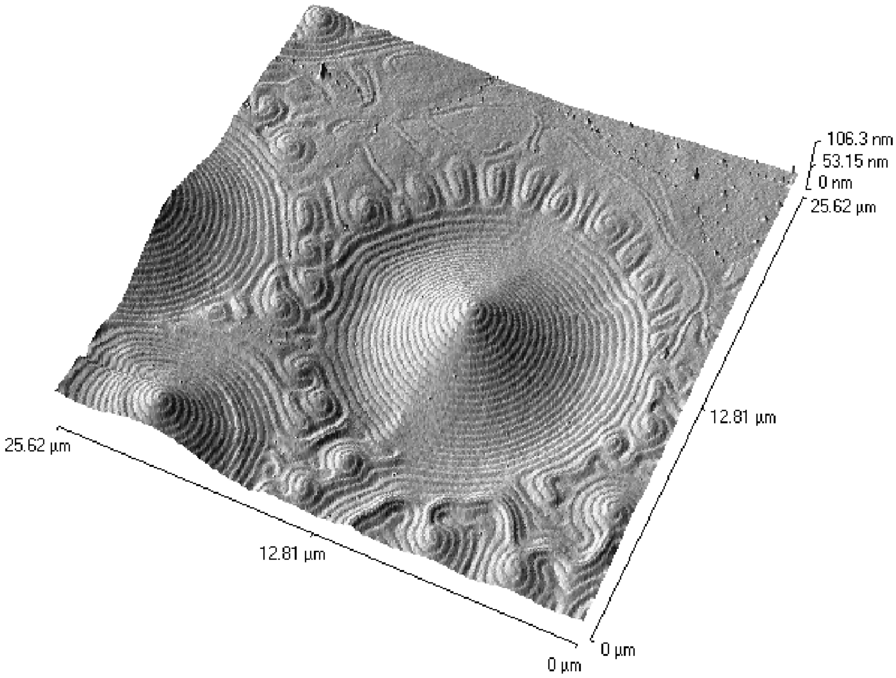

Figure 11. AFM image of hilly focal-conic domains (height ≈ 90 nm and line period ≈ 330 nm) of the cholesteric siloxane C4770L.

References

[1] Schmalfuss, H., Shen, D., Tschierske, C., and Kresse, H., 1999, *Liq. Cryst.*, **26,** 1767.

[2] Schönhals, A., and Kremer, F., 1994, *J. non-cryst. Solids*, **172–174,** 336.

[3] Kresse, H., 1983, *Advances in Liquid Crystals*, Vol. 6, edited by G. H. Brown (Academic Press), p. 109.

[4] Schmalfuss, H., Hauser, A., and Kresse, H., *Mol. Cryst. liq. Cryst.* (in the press).

[5] Saupe, A., 1995, *Arbeitsgruppe Flüssigkristalline Systeme an der Martin-Luther-Universität Halle*, in *MPG Jahrbuch 1995*, edited by Generalverwaltung der MPG München (Göttingen: Vandenhoeck & Ruprecht,), pp 739–740.

[6] Thieme, M., 1997, *Rasterkraftmikroskopische Untersuchungen freier Oberflächen von thermotropen Flüssigkristallen im Glaszustand*, Diss. Univ. Halle-Wittenberg, Ed. Wissenschaft, Reihe Chemie, Bd. 129, (Marburg: Tectum Verl.).

[7] Bouligand, Y., 1998, *Handbook of Liquid Crystals*, Vol. 1, edited by D. Demus, J. Goodby, G. W. Gray, H.-W, Spiess and V. Vill (Weinheim: Wiley-VCH), pp. 406–453.

[8] Oswald, P., 1994, *Solid State Phenom*, **35–36,** 121.

[9] Friedel, G., and Grandjean, F., 1910, *Bull. Soc. Fr. Miner.*, **33,** 409.

[10] De Gennes, P. G., and Prost, J., 1993, *The Physics of Liquid Crystals*, 2nd Edn (Oxford: Clarendon Press), pp. 466–506; Gray, G. W., and Goodby, J. W., 1984, *Smectic Liquid Crystals* (Glasgow and London: Leonard Hill).

[11] Pelzl, G., Diele, S., Grande, S., Jakli, A., Lischka, Ch., Kresse, H., Schmalfuss, H., Wirth, I., and Weissflog, W., 1999, *Liq. Cryst.*, **26,** 401.

[12] Meister, R., Hallè, M.-A., Dumoulin, H., and Pieranski, P., 1996, *Phys. Rev. E*, **54,** 3771.